IEEE Access
Multidisciplinary | Rapid Review | Open Access Journal

IEEE SYSTEMS, MAN AND CYBERNETICS SOCIETY SECTION

Received 10 June 2024, accepted 16 July 2024, date of publication 29 July 2024, date of current version 8 August 2024.

Digital Object Identifier 10.1109/ACCESS.2024.3435134

RESEARCH ARTICLE

Disturbance Attenuation-Based Global Integral Sliding Mode Control of an Electro-Hydraulic System With Prescribed Performance

VAN DU PHAN[1], PHUONG HO SY[1], AND KYOUNG KWAN AHN[2], (Senior Member, IEEE)
[1]School of Engineering and Technology, Vinh University, Vinh 43108, Vietnam
[2]School of Mechanical and Automotive Engineering, University of Ulsan, Ulsan 44610, South Korea

Corresponding author: Kyoung Kwan Ahn (kkahn@ulsan.ac.kr)

This work was supported by the 2023 Research Fund of University of Ulsan.

ABSTRACT The uncertainties and external disturbances inevitably reduce the displacement tracking efficiency of an electro-hydraulic system (ELHS). In this paper, the design of observer-based global integral sliding mode control is proposed for an electro-hydraulic system to eliminate the influences of the above-mentioned issues. Firstly, the mathematical model of the ELHS is established in canonical form to compound the impact of lumped disturbances. Then, the enhanced disturbance observer (EDO) is developed to tackle the lumped disturbances with the purpose of ameliorating estimation performance. Furthermore, a global integral sliding-mode surface integrated prescribed performance function is developed, with the goal of boosting global robustness, reducing chattering, and mitigating the significant effects of estimated disturbances error. The evidence of stability is ensured by deploying the Lyapunov principle, and the achievement of finite-time convergence of the ELHS has been attained. By comparing the proposed strategy with other controllers, the comparative experimental studies demonstrate the effectiveness and probability of the suggested method.

INDEX TERMS Enhanced disturbance observer, electro-hydraulic system, prescribed performance, global integral sliding mode control.

I. INTRODUCTION

A high-performance electro-hydraulic control system is crucial due to its wide application in various heavy-duty equipment used across industrial sectors, including automotive technology [1], excavators [2], hydraulic robotic arms [3], EHA load testers [4], and other fields [5]. The electro-hydraulic actuators (ELHSs) possess advantages such as energy efficiency, compact design, safety and reliability features, and variable speed and large force capability [6], [7], [8]. However, owing to various uncertainties and disruptions, achieving high precise tracking control of ELHS is challenging. Moreover, overcoming the effects of adverse factors and simultaneously obtaining the desired performance to bound tracking errors, finite-time convergence for the ELHS adds further difficulty.

The associate editor coordinating the review of this manuscript and approving it for publication was Huiyan Zhang.

To ensure satisfactory tracking performance, there exists two approaches: the states of the system in the given constraint space and the tracking error states transient performance criteria. The former often combines the barrier lyapunov function with backstepping technique to avoid the violating of the states with the predefined boundary [9], [10]. Meanwhile, the latter utilizes specified performance control [11] and constrained control, known as funnel control [12], [13]. It is noteworthy that the error boundary is unavailable in practice, therefore, the PPC is widely adopted to address this issue. In [14], Sui et al. investigated an adaptive prescribed performance control scheme for an uncertain non-strict feedback system, and a fuzzy inference system is deployed to tackle the unknown dynamic function. Xu et al. suggested an innovative backstepping technique approach for EHLS tracking control in [15], constructed to satisfy both conditions without violating any constraints and the prescribed transient tracking performance. Nevertheless, the integrated PPC to

the main controller in the presence of the uncertainties and disruptions is rately to ensure the convergence of error states with minor overshoots, and needs to solve.

Over the past few decades, numerous observer-based advanced control algorithms explored to boost control performance of ELHSs. In these approaches, the lumped disturbance, for instance, external load, unknown nonlinearities significantly affecting the control performance, is estimated, then, provided to main controller with the purpose of effectively compensated disturbances. Another approach, known as, big control coeficients is applied to enhance control action, sometimes resulting in instability. Hence, particularly noteworthy is an observation system, for instance, nonlinear disturbance observer (DO) [16], [17] a time-delay estimation interpretation [18], finite-time disturbance observer [19], [20], adaptive observer [21], extended sliding mode observer [22], [23], exact disturbance estimators [24]. To be specific, for improving the performance of the ELHS, nonlinear DO-based adaptive prescribed performance technology was utilized to approximate and compensate the uncertain part [25]. In [26], Mi et al. introduced a robust disturbance compensation displacement approach with control input constraints based on a linear extended state observer (ESO) to attenuate the extrinsic perturbation, deadzones nonlinearity, the severe supply pressure fluctuation, and various uncertainties without satisfying the prescribed performance. To this end, an enhanced disturbance observers (EDO) incorporated with numerouss control strategies is proposed to increase the proficiency of the position control loop. The EDO contains ESO and an adaptive law, used to obtain system state approximations and lumped disturbances. The ESO appraises the lumped disturbances as an extended state, which is estimated and compensated in the control law. Meanwhile, the adaptive law in EDO is adopted to improve the estimation performance. However, the innovative observer-based controller approaches has not been obtained the finite-time settling of the system states.

Several approaches have been developed to attain the finite-time convergence for ELHS such as terminal sliding mode control (TSMC) [27], finite-time backstepping-based feedback control [28], [29], global integral SMC [30], [31]. The system's rapid convergence to an equilibrium point is ensured by the inclusion of an adjustable exponential term in the finite-time control (FiTC). Motivated by the unique merits of FiTC, Zhang et al. [31] suggested a global sliding mode FiTC scheme for a hydraulic roofbolter systems. The authors in [32] presented the disturbance observer-based backstepping FiTC to not only cope with the inconsistency and approximation errors but also ensure the finite-time pursuing for ELHS toward the target signal. Alternatively, [33] proposed a dynamic surface quasi-synchronization technique combining a terminal sliding mode observer for the ELHS subject to external load disturbance and parametric uncertainty, where the outputs constraint was met by barrier Lyapunov function. Nonetheless, only estimation error converges in a limited time without experimental validation in these reported methods. Therefore, investigating both FiTC and experimental verifications under lumped distubances envolves this article.

Attracted by the preceding drawback, the proposed strategy in this paper for an ELHS is investigated by employing the GISMC integrated PPC and EDO that guarantees the system steadiness and constraint situation considering lumped uncertainties. It is worthwhile mentioning that the limited studies effort to handle uncertainties and external disturbances but bring the prescribed performance and finite-time convergence for ELHSs. In comparison to prior studies, the advantages of this article can be evaluated as follows:

1) This work firstly simultaneously solve the lumped disturbances, prescribed tracking performance and finite-time convergence for the ELHS. This aspect enhances the practical feasibility of the designed controller for real-world applications

2) To efficiently mitigate the impacts of the lumped disturbance in the ELHS, the EDO is developed with the purpose of ameliorating estimation performance.

3) The suggested method based on the global intergral sliding mode approach with prescribed performance is conducted to enhance the output tracking precision and guarantee the output position within arbitrary boundaries amidst external influences.

4) The system stability and finite-time tracking error convergence are validated using the Lyapunov approach, and the capability and productivity of the proposed strategy are confirmed through experimental results.

The organization of this article is as follows: Section II presents the mathematical model of the ELHS including the problem descriptions and several assumptions. The procedure of proposed method is outlined in section III. Sections IV shows the experiment studies. Ultimately, Section V summarizes the conclusions.

II. PROBLEM DESCRIPTION

The technical drawing of the ELHS in this paper is illustrated in Fig. 1. The ELHS contains a double-rod cylinder, a servo valve, a relief valve, an AC motor and a pump, a displacement sensor, two pressure transducers, and a controller with AD/DA. The following section discusses the mathematical model of a class of ELHS.

The dynamics of the ELHS can be formulated by the law of acceleration.

$$\begin{aligned} m\ddot{x} &= P_{Lo}A - B\dot{x} + d\,(t, x, \dot{x}) \\ Q_L &= k_t u\sqrt{P_s - sign\,(u)\,P_{Lo}} \\ \dot{P}_{Lo} &= \frac{4\beta_e}{V_c}\,(Q_L - q_L + Q_{Li}) - \frac{4\beta_e A}{V_c}\dot{x} \end{aligned} \tag{1}$$

where x, m, and B define the piston's displacement, mass of the moving component, and viscous damping factor, respectively; $d(\bullet)$ describes the disturbance variables such as external force, friction; $P_{Lo} = P_1 - P_2$ represents the load pressure, with P_1, P_2 being the pressure of each chamber, P_s defines the supply pressure, k_t is a proportional coefficient of the

servo-valve, and $sign(\bullet)$ is a signum function. β_e, A are the Bulk modulus, a piston cross-sectional area, respectively. $q_L = C_0 P_{Lo}$ denotes the internal leakage, C_0 is the nominal coefficient. V_c is a constant cylinder control volume. The dynamic error model, Q_{Li}, contains uncertainties, lumped modeling error, etc.

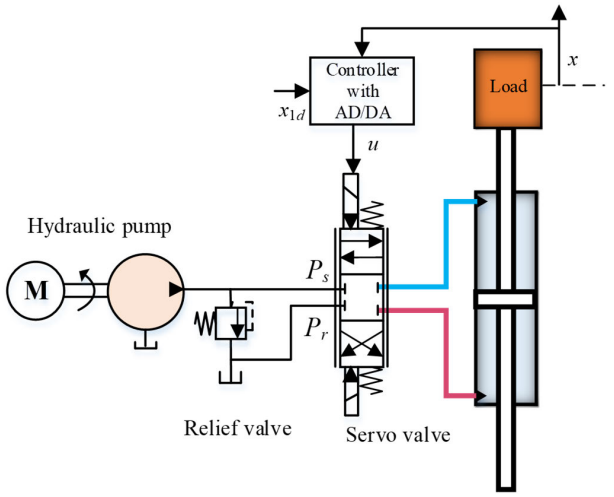

FIGURE 1. The technical drawing of the ELHS.

From (1), it can be represented as follows:

$$x = \frac{4\beta_e A k_t}{V_c m} u\sqrt{P_s - sign(u) P_{Lo}} - \frac{4\beta_e}{V_c}\frac{A}{m} C_0 P_{Lo} - \frac{4\beta_e A^2}{V_c m}\dot{x} - \frac{B}{m}\ddot{x} + \frac{\dot{d}}{m} + \frac{4\beta_e A}{V_c m} Q_{Li} \tag{2}$$

Choosing $\varepsilon = [\varepsilon_1, \varepsilon_2, \varepsilon_3]^T \triangleq [x, \dot{x}, \ddot{x}]^T$ as the state variables. From (1)–(2), the ELHS model can then be re-written as follows:

$$\begin{cases} \dot{\varepsilon}_1 = \varepsilon_2 \\ \dot{\varepsilon}_2 = \dot{\varepsilon}_3 \\ \dot{\varepsilon}_3 = h(\varepsilon_2, \varepsilon_3) + g(\varepsilon_3, u) u + \Delta(t) \\ y = \varepsilon_1 \end{cases} \tag{3}$$

where

$$g = \frac{4\beta_e A k_t}{V_c m}\sqrt{P_s - sign(u) P_{Lo}}, \Delta = \frac{\dot{d}}{m} + \frac{4\beta_e A}{V_c m} Q_{Li}$$
$$h = -\frac{4\beta_e}{V_c}\frac{A}{m} C_0 P_{Lo} - \frac{4\beta_e A^2}{V_c m}\varepsilon_2 - \frac{B}{m}\varepsilon_3,$$

Remark 1: The control aim is to faithfully synthesize an adaptive observer-based GTSMC algorithm for the plant (3) such that

1) The output displacement ε_1 precisely follows the desired trajectory ε_{1d} in which the tracking error is ensured to prescribed performance specifications and finite-time convergence;

2) The enhanced disturbance observer tracking error converges to a bounded region in a certain time.

In order to assist the control objective, various assumptions and lemmas are given as follows:

Assumption 1: a) The tracking target signal ε_{1d} and its derivative $\dot{\varepsilon}_{1d}$ are bounded.

b) There exist upper bounds for Δ_1, Δ_2 and their derivatives $\dot{\Delta}_1$, $\dot{\Delta}_2$ such that they satisfy $|\Delta_i| \leq d_{im}$, $|\dot{\Delta}_i| \leq D_i$; $i = 1, 2$, in which d_{im}, D_i, are positive terms.

Lemma 1 ([10], [34]): Consider a nonlinear system $\dot{x} = f(x)$. $V(x)$ is positive definite, continuous and smooth function. If the existing inequality satisfies:

$$\dot{V}(x) \leq -H_1 V(x) - H_2 V^{\beta}(x) + C^* \tag{4}$$

where υ, H_1, H_2, C^* are the positive constants with $0 < \upsilon < 1$ and $0 < C^* < \infty$, then, the ballance points of the presented system $\dot{x} = f(x)$ is practical finite-time stable, and the convergence time T holds

$$T \leq T_p = \max\left\{ t_0 + \frac{1}{\lambda_0 H_1 (1-\upsilon)} \ln \frac{\lambda_0 H_1 V^{1-\upsilon}(t_0) + H_2}{H_2} \times t_0 + \frac{1}{H_1 (1-\upsilon)} \ln \frac{H_1 V^{1-\upsilon}(t_0) + \lambda_0 H_2}{\lambda_0 H_2} \right\} \tag{5}$$

where $0 < \lambda_0 < 1$. The system state x will be guided into the compact set that can be defined by

$$x \in \left\{ x: \lim_{t \to T_p} V(x) \leq \min\left\{ \frac{C^*}{(1-\lambda_0) H_1}, \left(\frac{C^*}{(1-\lambda_0) H_2}\right)^{\frac{1}{\upsilon}} \right\} \right\} \tag{6}$$

III. CONTROLLER DESIGN

A. ENHANCED DISTURBANCE OBSERVER DESIGN

The organization of suggested controller is depicted in Fig. 2, which contains two main parts: EDO and GISMC with PPF.

Define $\dot{\Delta}(t) = \Delta_d(t)$. The equation (3) can be re-expressed as follows:

$$\begin{cases} \dot{\varepsilon}_1 = \varepsilon_2 \\ \dot{\varepsilon}_2 = \varepsilon_3 \\ \dot{\varepsilon}_3 = h(\varepsilon_2, \varepsilon_3) + g(\varepsilon_3, u) u + \varepsilon_d(t) \\ \dot{\varepsilon}_d(t) = \Delta_d(t) \end{cases} \tag{7}$$

Define $\tilde{\varepsilon}_i = \varepsilon_i - \hat{\varepsilon}_i$. The enhanced disturbance observer (EDO) are constructed as follows:

$$\begin{cases} \dot{\hat{\varepsilon}}_1 = \hat{\varepsilon}_2 + 4L_1\tilde{\varepsilon}_1 \\ \dot{\hat{\varepsilon}}_2 = \hat{\varepsilon}_3 + 6L_1^2\tilde{\varepsilon}_1 \\ \dot{\hat{\varepsilon}}_3 = h(\varepsilon_2, \varepsilon_3) + g(u) u + \hat{\varepsilon}_d(t) + 4L_1^3\tilde{\varepsilon}_1 \\ \dot{\hat{\varepsilon}}_d(t) = L_1^4\tilde{\varepsilon}_1 + \hat{\beta}_d sign(\sigma_d) \end{cases} \tag{8}$$

where $L_1 > 0$ is the constant coeficient, $\hat{\varepsilon}_i$ $(i = 1,2,3, d)$ is the estimatied value of ε_i, σ_d is function gain and designed later.

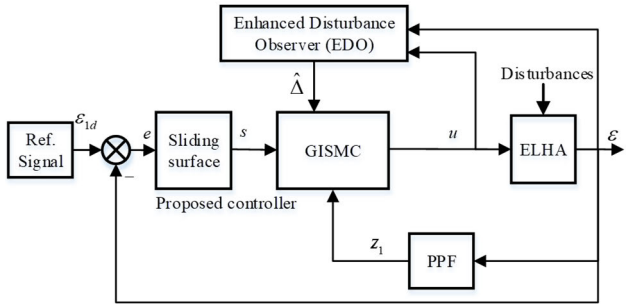

FIGURE 2. Overview of the proposed control method.

From (7) and (8), the differential equation of the observation error can be represented by:

$$\begin{cases} \dot{\tilde{\varepsilon}}_1 = \tilde{\varepsilon}_2 - 4L_1\tilde{\varepsilon}_1 \\ \dot{\tilde{\varepsilon}}_2 = \tilde{\varepsilon}_3 - 6L_1^2\tilde{\varepsilon}_1 \\ \dot{\tilde{\varepsilon}}_3 = \tilde{\varepsilon}_d(t) - 4L_1^3\tilde{\varepsilon}_1 \\ \dot{\tilde{\varepsilon}}_d(t) = \Delta_d - L_1^4\tilde{\varepsilon}_1 - \hat{\beta}_d \text{sign}(\sigma_d) \end{cases} \tag{9}$$

where $\hat{\beta}_d$ are the estimated value of β_d, which is the designed adaptive gain.

Letting $\eta = [\eta_1, \eta_2, \eta_3, \eta_d]^T = \left[\tilde{\varepsilon}_1, \tilde{\varepsilon}_2/L_1, \tilde{\varepsilon}_3/L_1^2, \tilde{\varepsilon}_d/L_1^3\right]^T$ as the scaled estimation error vector, (9) can be described as follows:

$$\begin{cases} \dot{\eta}_1 = L_1\eta_2 - 4L_1\eta_1 \\ \dot{\eta}_2 = L_1\eta_3 - 6L_1\eta_1 \\ \dot{\eta}_3 = L_1\eta_4 - 4L_1\eta_1 \\ \dot{\eta}_d(t) = -L_1\eta_1 + \left(\Delta_d - \hat{\beta}_d \text{sign}(\sigma_d)\right)/L_1^3 \end{cases} \tag{10}$$

We can express the time derivative of η as follows:

$$\begin{cases} \dot{\eta} = L_1 M_0 \eta + K_0 \delta \\ y = C\eta \end{cases} \tag{11}$$

where M_0, K_0, and C are designed matrices and described as follows:

$$M_0 = \begin{bmatrix} -4 & 1 & 0 & 0 \\ -6 & 0 & 1 & 0 \\ -4 & 0 & 0 & 1 \\ -1 & 0 & 0 & 0 \end{bmatrix}, K_0 = \begin{bmatrix} 0 \\ 0 \\ 0 \\ 1 \end{bmatrix},$$
$$\delta = \left(\Delta_d - \hat{\beta}_d \text{sign}(\sigma_d)\right)/L_1^3, C = \begin{bmatrix} 1 & 0 & 0 & 0 \end{bmatrix} \tag{12}$$

As M_0 is Hurwitz, a positive definite matrix Z_o is introduced to guarantee $M_o^T Z_o + Z_o M_o = -2Q$, in which Q is positive definite matrix such as a unit matrix. Hence, the matrix Z_o can be deduced as:

$$Z_0 = \frac{1}{8}\begin{bmatrix} 17 & -4 & -11 & 4 \\ -4 & 11 & -4 & -17 \\ -11 & -4 & 17 & -4 \\ 4 & -17 & -4 & 91 \end{bmatrix} \tag{13}$$

The adaptive gain $\hat{\beta}_d$ can be designed by

$$\dot{\hat{\beta}}_d = \frac{\alpha_1}{L_1}\eta^T Z_0 K_0 sign(\sigma_d) \text{ or} \hat{\beta}_d$$
$$= \frac{\alpha_1}{L_1}\int_0^t \eta^T Z_0 K_0 sign(\sigma_d) d\tau \tag{14}$$

where $\alpha_1 > 0$ is a tunable parameter, $\sigma_d = \eta^T Z_0 K_0$ with β_d ensures the following term

$$\beta_d > \bar{\Delta}_1 \tag{15}$$

where $\bar{\Delta}_1$ are the the upper bound of Δ_d.

Remark 2: From (14), the real time value $\hat{\beta}_d$ can be achieved by integrating both sides of (14), which is described by [21], [24].

$$\hat{\beta}_d = \frac{1}{2}\frac{\alpha_1}{L_1}\left[\frac{3}{L_1}|\eta_1| + 5\int_0^t |\eta_1(\tau)| d\tau\right] \tag{16}$$

Theorem 1: With the ELHS (3), the EDO is designed in (8) and choosing observer gain L_1 and α_1 large enough, then the observer error signals are bounded as $t \to \infty$.

Proof:

Take into account the Lyapunov function

$$V_{EDO} = \frac{1}{2}\eta^T Z_0 \eta \tag{17}$$

where Z_o is a positive definite matrix.

The time derivative of V_{EDO} is calculated by

$$\dot{V}_{EDO} = \frac{1}{2}\dot{\eta}^T Z_0 \eta + \frac{1}{2}\eta^T Z_0 \dot{\eta} \tag{18}$$

Substituting (11) into (18) gets:

$$\begin{aligned} \dot{V}_{EDO} &= \frac{1}{2}(L_1 M_0 \eta + K_o\delta)^T Z_0 \eta + \frac{1}{2}\eta^T Z_0 (L_1 M_0 \eta + K_0\delta) \\ &= \frac{1}{2}L_1 (M_0\eta)^T Z_0 \eta + \frac{1}{2}L_1 \eta^T Z_0 M_0 \eta + \eta^T Z_0 K_0 \delta \\ &= \frac{1}{2}L_1 \eta^T \left(M_0^T Z_0 + Z_0 M_0\right)\eta + \eta^T Z_0 K_0 \delta \\ &= -L_1 \eta^T \eta + \eta^T Z_0 K_0 \delta \\ &= -L_1 \eta^T \eta + \eta^T Z_0 K_0 \left(\Delta_d - \hat{\beta}_d \text{sign}(\sigma_d)\right)/L_1^3 \\ &= -L_1 \eta^T \eta + \eta^T S_0 \end{aligned} \tag{19}$$

where S_o is defined by $S_0 = Z_0 K_0 \left(\Delta_d - \hat{\beta}_d \text{sign}(\sigma_d)\right)/L_1^3$.

Assume $\|S_0\|_4$ is bounded and $\|S_0\|_4 \leq \mu_1 \lambda_{max}(Z_0 K_0) \|\eta\|_4$, we can obtain

$$\dot{V}_{EDO} \leq -\left(1 - \frac{\mu_1 \lambda_{max}(Z_0 K_0)}{L_1}\right)\eta^T \eta \tag{20}$$

If the following inequality $\mu_1 \lambda_{max}(Z_0 K_0) < L_1$ holds, it implies that $\dot{V}_{EDO}$ is negative definite. As $V_{EDO} > 0$, $\dot{V}_{EDO} \leq 0$. Thus, it can be deduced that all error estimation of the designed EDOs can be concluded as bounded, i.e. $\tilde{\varepsilon}_1 \leq \varepsilon_{1m}, \varepsilon_{1m} > 0$. The proof is completed.

B. COMPOSITE CONTROL DESIGNS

Expanding on the foundational technical lemmas and crucial functions discussed in the previous two sections, a of observer-based global sliding mode control PPC approach is crafted by integrating EDO and global integral sliding

mode control techniques. The subsequent analysis focuses on ensuring the stability of the control system.

The error state is defined as follows:

$$e = \varepsilon_1 - \varepsilon_{1d}; \tag{21}$$

where ε_{1d} is the desired signal of the output position.

Definition 1: A continuous function is presented as the prescribed performance function (PPF) [14]: $\rho(t) = (\rho_0 - \rho_\infty)e^{-ct} + \rho_\infty$ where $c > 0$ denotes the convergence rate, ρ_0 and ρ_∞ describes the initial state of PPC and the allowable steady-state values, which satisfies the initial conditions $\rho(t) = \rho_0 > 0$ as $t \to 0$, $\rho(t) = \rho_\infty > 0$ as $t \to \infty$, and $\rho_0 > \rho_\infty$.

Hence, the tracking error of output position lies in the boundnesss of the PPC by the following inequality

$$-\varsigma_d \rho(t) < e < \varsigma_u \rho(t), t > 0 \tag{22}$$

where ς_d and $\varsigma_u > 0$ are the designed constants.

The following function $G(z_1)$ of the tracking error e is used to further increase the convergence of e which is presented as follows:

$$G(z_1) = \frac{\varsigma_u e^{z_1} - \varsigma_d e^{-z_1}}{e^{z_1} + e^{-z_1}} \tag{23}$$

where $z_1 \in R$, and $G(z_1) \in (-\varsigma_d, \varsigma_u)$.

The index function of the tracking error e to restrict it can be selected as follows:

$$e = \rho G(z_1) \tag{24}$$

Based on the definition 1, prescribed performance is tailored to construct the transformation errors. Given that $G(z_1)$ is strictly monotonically increasing, and prescribed performance parameters are chosen to meet $0 < \rho_\infty < \rho(t) < \infty$, we can therefore derive an inverse transfer function z_1 as follows:

$$z_1 = G^{-1}\left(\frac{e}{\rho}\right) = \frac{1}{2}\ln\left(\varsigma_d + \frac{e}{\rho}\right) - \frac{1}{2}\ln\left(\varsigma_u - \frac{e}{\rho}\right) \tag{25}$$

It is noted that the original tracking error e is converted by the smooth function $G(z_1)$, as seen that z_1 will tend to infinity when e reaches the boundary $(-\varsigma_d\rho, \varsigma_u\rho)$. Therefore, the tracking error signal e lies in the boundness of PPC (22) [31], [37].

According to the canonical form of the EHS mathematical model, the integral sliding surface is formulated as

$$s = \hat{\varepsilon}_3 + 2\kappa_0 z_1 + \kappa_0^2 \int_0^t z_1 d\tau - p(t) \tag{26}$$

where $\kappa_0 > 0$, $p(t) = p(0)\exp(-\kappa_{10}t)$, $p(0) = \hat{\varepsilon}_3(0) + 2\kappa_0 z_1(0) + \kappa_0^2 \int_0^t z_1(0)\, d\tau$.

Then, the time derivative of s signal are computed as follows:

$$\dot{s} = \dot{\hat{\varepsilon}}_3 + 2\kappa_0 \dot{z}_1 + \kappa_0^2 z_1 - \dot{p}(t) \tag{27}$$

Substituting (29) to (31), we obtain

$$\dot{s} = h + gu + \hat{\varepsilon}_d(t) + 4L_1^3\tilde{\varepsilon}_1 + 2\kappa_0\dot{z}_1 + \kappa_0^2 z_1 - \dot{p}(t) \tag{28}$$

From (28), the control signal can be elaborated as follows:

$$u = \frac{1}{g}\left(-h - 2\kappa_0\dot{z}_1 - \kappa_0^2 z_1 + \dot{p}(t) - \hat{\varepsilon}_d - \kappa_2 s - \kappa_1 sign(s)\right) \tag{29}$$

where κ_1 and $\kappa_2 > 0$ are the positive designed parameters.

Theorem 2: With the ELHS (3), under Assumption 1, Lemma 1, the designed observer is introduced in (8), the PPC is suggested in (22), and the final control law is constructed in (29). Hence, all system states are bounded, and the tracking errors converge to the predefined-boundary.

Proof:

Take into account the Lyapunov function

$$V_1 = \frac{1}{2}s^2 \tag{30}$$

where Z_o is a positive definite matrix.

The time derivative of V_1 is calculated by

$$\begin{aligned}\dot{V}_1 &= s\dot{s} \\ &= s\left(h + gu + \hat{\varepsilon}_d(t) + 4L_1^3\tilde{\varepsilon}_1 + 2\kappa_0\dot{z}_1 + \kappa_0^2 z_1 - \dot{p}(t)\right)\end{aligned} \tag{31}$$

Substituting (29) to (31), we attain

$$\dot{V}_1 = s\dot{s} = -\kappa_1|s| - \kappa_2 s^2 - 4sL_1^3\tilde{\varepsilon}_1 \tag{32}$$

Applying Young's inequality, one obtains

$$-4sL_1^3\tilde{\varepsilon}_1 \le s^2 + 4L_1^6\varepsilon_{1m}^2 \tag{33}$$

From (32) to (33), we attain

$$\begin{aligned}\dot{V}_1 = s\dot{s} &= -\kappa_1|s| - (\kappa_2 - 1)s^2 + 4L_1^6\varepsilon_{1m}^2 \\ &= -\kappa_1 V_1^{\frac{1}{2}} - (\kappa_2 - 1)V_1 + C_0\end{aligned} \tag{34}$$

Following to Lemma 1, the errors states of the ELHS will be pushed on the sliding mode $s = 0$ within a predefined time T_c. The finite-time T_c is computed as given by the equation (5).

IV. COMPARATIVE STUDY OF SIMULATION AND EXPERIMENTS

To demonstrate the improved proficiency of the indicated methodology, the comparative study of simulation and experiments are performed in the ELHS by using Matlab/Simulink (R2022a version). The sinusoidal signal is considered as the reference signal in the simulation. Meanwhile, the desired signal, i.e., the square signal, sinusoidal signal, and chirp input signal, are carried out in the experiment scenarios.

The physical parameters of the ELHS are given based on the reference [38] as itemized in Table 1.

The following four control strategies are given and compared to prove the availability and outstanding tracking efficiency of the suggested methodology in various experiments.

C1: Strategy 1 is ASMC [6] that combine the adaptive law and sliding mode control techniques. The final

TABLE 1. Electro-hydraulic system parameters.

Symbol	Description	Value (unit)
β_e	Bulk modulus factor	$1.25\text{x}10^3$ (MPa)
k_t	Valve coefficient	$3.2\text{x}10^{-8}$ ($m^3/s/V/Pa^{-1/2}$)
B	Friction coefficient	450 (Ns/m)
m	Mass of cylinder	4.5 (kg)
A	Work area	$4\text{x}10^{-4}$ (m^2)
P_s	Supply pressure	16 (MPa)
P_r	Return pressure	0.1 (MPa)
V_c	Control volume	$6\text{x}10^{-5}$ (m^3)
C_0	Leakage coefficient	$1.2\text{x}10^{-11}$ (m^5/Ns)

control law of this controller can be designed as follows: $u = (S_cB)^{-1}\left[S_c\dot{X}_d - S_cA\hat{X} - k_s\text{sgn}(\hat{s})\right] - \hat{\Delta}$, $S_c = \left[\lambda^2\ 2\lambda\ 1\right], X_d = \left[\varepsilon_{1d}\ \dot{\varepsilon}_{1d}\ \ddot{\varepsilon}_{1d}\right], X = \left[x\ \dot{x}\ \ddot{x}\right], s = S_c\,(X - X_d)$

C2: Strategy 2 is BCESO [39] that combine the backstepping control and dual extended state observer. The final control law of this controller can be designed as follows: $u = \frac{1}{g}\left(-h - \hat{\Delta} + \dot{\alpha}_2 - k_3e_3\right)$,

C3: Strategy 3 is PID [9] with the following control law: $u = K_pe + K_d\dot{e} + K_i\int_0^t e\,(t)\,dt$

C4: Strategy 4 is PIDFF [40] PID with feed-forward velocity. The control law of this controller can be designed as follows: $u = K_pe + K_d\dot{e} + K_i\int_0^t e\,(t)\,dt + K_v\dot{\varepsilon}_{1d}$

Proposed controller: Strategy 5 is AESO-GISMC with PPC.

The prescribed performance functions (PPF) are selected as $PPC^+(t) = 4\pi e^{-2t} + 1.5$ mm and $PPF^-(t) = -PPF^+(t)$. The control parameters and observer parameters of the various controllers are carefully adjusted and tuned by empirical method. Then, the compared controllers' parameters are described in Table 2.

Remark 3: For the experiment, to capture velocity and acceleration data, we utilize a second-order exact differentiation [35], in the following manner:

$$\begin{aligned}
\dot{\chi}_0 &= \upsilon_0 \\
\upsilon_0 &= -\Gamma_1\left|\chi_0 - \varepsilon_1\right|^{2/3} sign\left(\chi_0 - \varepsilon_1\right) + \chi_1 \\
\dot{\chi}_1 &= \upsilon_1 \\
w_1 &= -\Gamma_2\left|\chi_1 - \upsilon_0\right|^{2/3} sign\left(\chi_1 - \upsilon_0\right) + \chi_2 \\
\dot{\chi}_2 &= -\Gamma_3 sign\left(\chi_2 - \upsilon_1\right)
\end{aligned} \tag{35}$$

where Γ_1, Γ_2, and Γ_3 are selected as appropriate positive parameters.

Subsequently, the information of velocity and acceleration can be attained as follows:

$$\chi_1 = \dot{\varepsilon}_1,\ \chi_2 = \ddot{\varepsilon}_1. \tag{36}$$

TABLE 2. Compared controllers' parameters.

Controllers	Parameters
ASMC	$k_1 = 5$, $k_s = 45$, $k_3 = 10$, λ=10
BCESO	$k_1 = 25$, $k_2 = 15$, $k_3 = 10$, $L = 40$.
PID	$K_p = 50$, $K_i = 10$, $K_d = 0.1$.
PIDFF	$K_p = 50$, $K_i = 10$, $K_d = 0.1$, $K_v = 60$,
Proposed	$\kappa_0 = 5$, $\kappa_1 = 35$, $\kappa_2 = 15$, $L_1 = 40$, $\alpha_1 = 0.1$.

A. SIMULATION RESULTS

The simulation was conducted to assess the superity of the proposed method under desired pulse signals with the external load test environment. The simulation results are described in Fig. 3. The tracking efficiency of the PID, PIDFF, proposed controller, ASMC, and BCESO controller are exhibited by the red lines, orange lines, purple lines, green lines, and blue lines, respectively. The control actions are confined within a range narrower than ± 10 V, indicating the viability of the proposed controller. We can see that the tracking error of the suggested control algorithm is the smallest and bouned in the PPF as compared to other four control algorithms. Fig. 4 exhibits the curves of lump disturbance estimation. As seen in Fig. 4, the proposed EDO provides the well tracking of the estimated disturbance and its actual value.

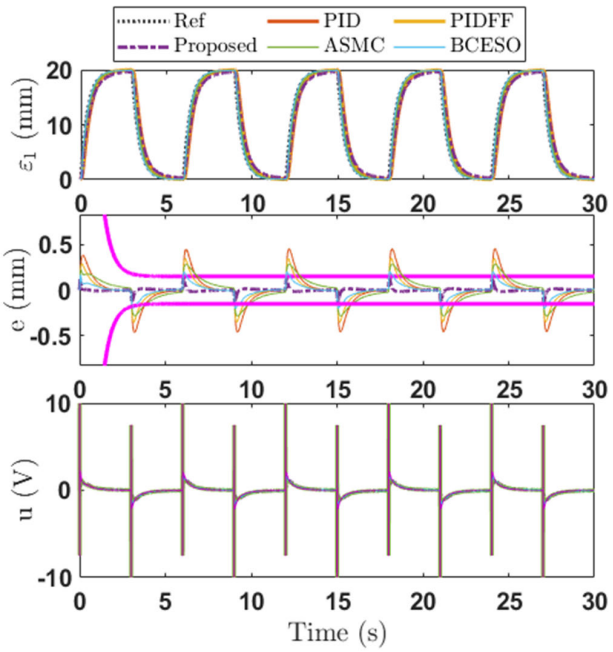

FIGURE 3. Efficiency of various control methods in simulation.

B. EXPERIMENT SETUP

The real-time ELHS testbench hardware is illustrated in Fig. 5. Meanwhile, the components setting of the practical

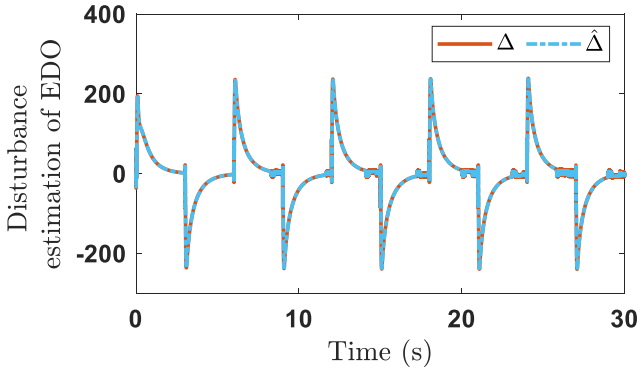

FIGURE 4. Estimatied lumped disturbance of the suggested method in simulation.

ELHS are reported in Table 3. Within this setup, a pump is powered by an AC motor (three phase, rated power 3.7 kW) and controlled by an inverter SIMATICS V20 housed in the control box. This pump facilitates the transfer of oil to a double-rod cylinder through a servo valve (MOOG − D633-317B), enabling the system to function. Precision control within the system is achieved with the aid of two pressure sensors and a position sensor SXM30, ensuring accurate and efficient operation. For data acquisition purposes, the system utilizes a PCI 6014 card equipped with terminal connectors, seamlessly integrated with an industrial computer. This computer is specifically configured with Matlab/Simulink software, enabling comprehensive monitoring, analysis, and control of the ELHS testbench operations.

C. EXPERIMENT RESULTS

Three experiments were conducted to assess the superity of the proposed method under various desired signals with the same test environment. Experiment 1 considered a square wave trajectory with an amplitute of 20 [mm] and a pulse width of 50%. Experiment 2 considered a sinusoidal trajectory with an maximum value of 20 [mm] and a frequency 0.5 Hz. Experiment 3 considered a a chirp input signal with an amplitute 20 [mm] and linear sweep from 0.5 to 1 Hz. The experiment results are described as follows.

Experiment 1: Figs. 6 − 8 depict the the experiment results in the first study, where Fig. 6 presents the curves of the output signal $x = \varepsilon_1$ and the given target trajectory ε_{1d}. In addition, the trajectories of control signals and tracking errors are also exhibited in the second and third subgraph of Fig. 6. The tracking efficiency of the PID control, PIDFF control, ASMC, BCESO, and the proposed control are displayed by the red lines, orange lines, green lines, blue lines, and purple lines, respectively. The control actions are confined within a range narrower than ± 10 V, indicating the viability of the proposed controller. Furthermore, it can be revealed from Fig. 6 that the system output of the various controllers can follow the given target trajectory well. The tracking errors of the ELHS with the suggeted methodology is little than these presented controllers because the proposed control laws are generated from the global integral SMC integrated EDO. By utilizing the ESO enhanced by adaptive law, the suggested algorithm control achieves the highest accuracy in the position tracking for ELHS. Furthermore, the suggested method Fig. 7 displays the zoom-in of the tracking error that falls within the specified performance condition. The curves of the two chambers's pressure are depicted in first subgraph of Fig. 7. Meanwhile, the second subgraph of Fig. 8 exhibits the curves of lump disturbance estimation.

TABLE 3. Components setting of the practical ELHS.

Devices	Descriptions	Specification
Double-rod cylinder	Type Stroke Tube diameter	Symmetrical actuator 25 [mm] 36 [mm]
AC motor	Type Rated output power Frequency Synchronous speed	Three phase 3.7 [kW] 50 [Hz] 1500 [rpm]
Inverter	Type Line voltage Rated power	Simatics V20 380 [V] 5.5 [kW]
Hydraulic pressure sensor	Type Supply power Output Range	MPM4150 12 – 24 [V] 0 – 10 [V] 0 – 30 [MPa]
Displacement sensor	Type Supply power Output Range	SXM30 12 – 24 [V] 0 – 10 [V] 0 – 50 [cm]
Servo valve	Manufacturer Output Supply power Max pressure	MOOG – D633-317B 0 to 10 [V] 24 [V] 35 [MPa]
Data acquisition Card	Type Resolution Analog input/output	NI PCI-6014 16-bits 16AI/2AO

Experiment 2: In this experiment, the ELHS operates in lumped disturbance condition with the desired time-varying reference signal is defined as follows:

$$\varepsilon_{1d}(t) = 10 + 10sin(0.5\pi t - \pi/2) \quad (\text{mm}) \tag{37}$$

Figs. 9 – 11 show the experiment results in the second study. The experimental data including actual output

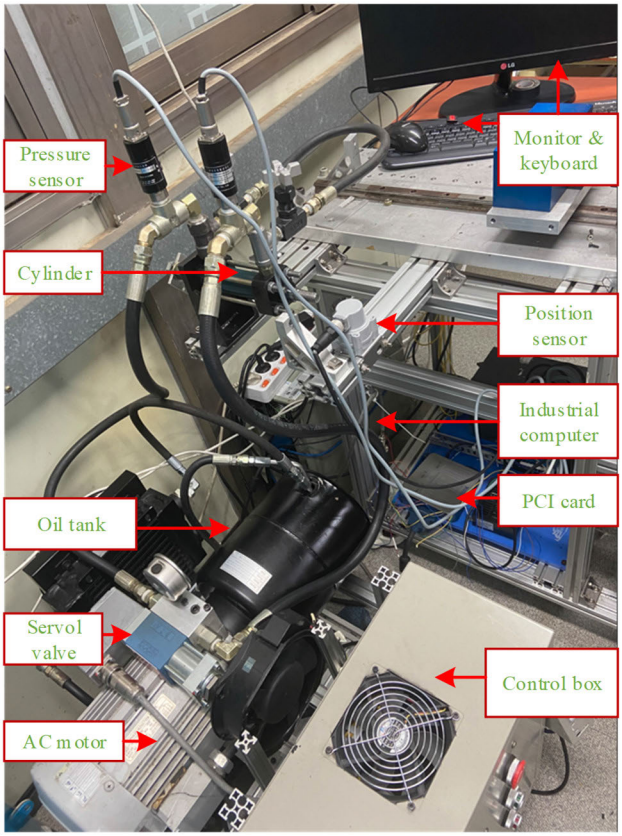

FIGURE 5. The experimental equipment of ELHS.

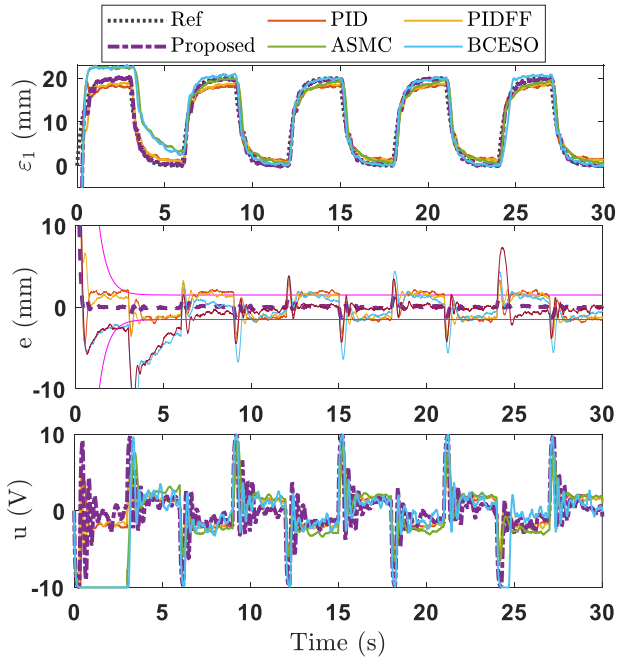

FIGURE 6. Efficiency of various control methods in experiment 1.

position and its reference, tracking error, and control action are depicted in Fig. 9. When compared to the baseline controllers, the suggested controller demonstrates adjustments in

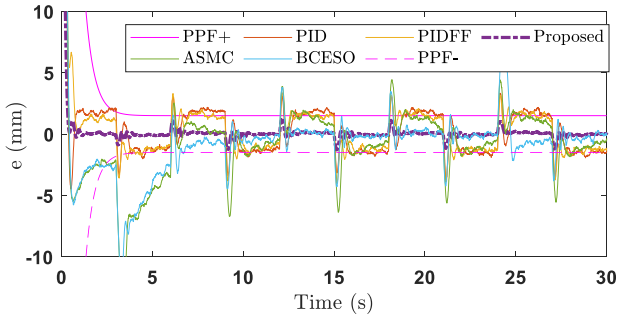

FIGURE 7. Tracking errors of various control methods in experiment 1.

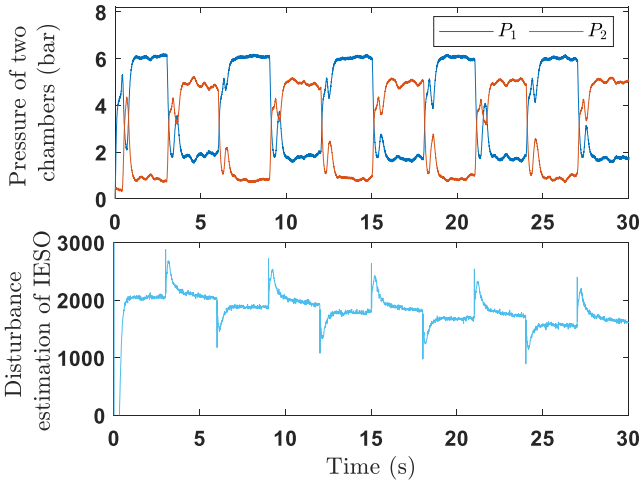

FIGURE 8. Pressure of two chamber and lumped disturbance of the suggested method in experiment.

tracking performance across both steady-state and transient stages. Furthermore, the suggested method steers the tracking error within the predefined PPC, eventually achieving the desired performance in tracking tasks. The enlarge of tracking errors is depicted in Fig. 10. Meanwhile, the pressure of two chambers and lumped disturbance of the suggested method in experiment are displayed in Fig. 11.

Experiment 3: In this scenario, the frequency of the desired signal is increased by twice. It can be described by

$$\varepsilon_{1d}(t) = 10\left(1 - \cos(\pi t)\right)\left(1 - e^{-t}\right) \text{ (mm)} \qquad (38)$$

Figs. 12 – 14 show the experiment results in the second study. The experimental data including position response, tracking error, and control action are depicted in Fig. 12. It implies that the proposed approach delivers superior control performance with the boudary of the tracking error. In contrast to the suggested method, which ensures the prescribed performance, the baseline approaches showcases weekness control performance. The tracking errors of comparative controller exceeds the prescribed performance regions. The enlarge of tracking errors is depicted in Fig. 13. Meanwhile, the pressure of two chambers and lumped disturbance of the suggested method in experiment are displayed in Fig. 14. The effectiveness and validity of the suggested control are clearly

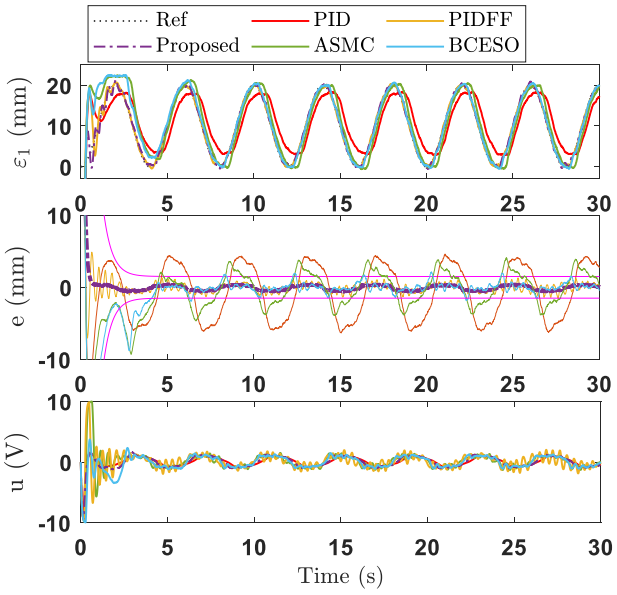

FIGURE 9. Efficiency of various control methods in experiment 2.

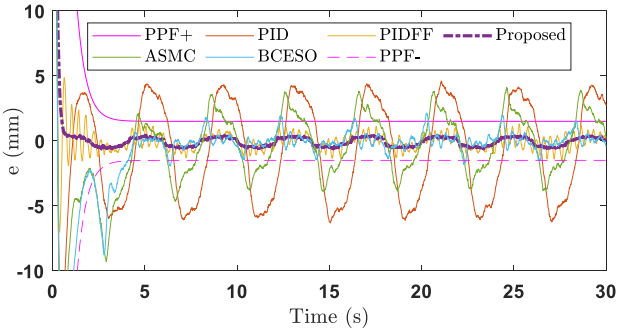

FIGURE 10. Tracking errors of various control methods in experiment 2.

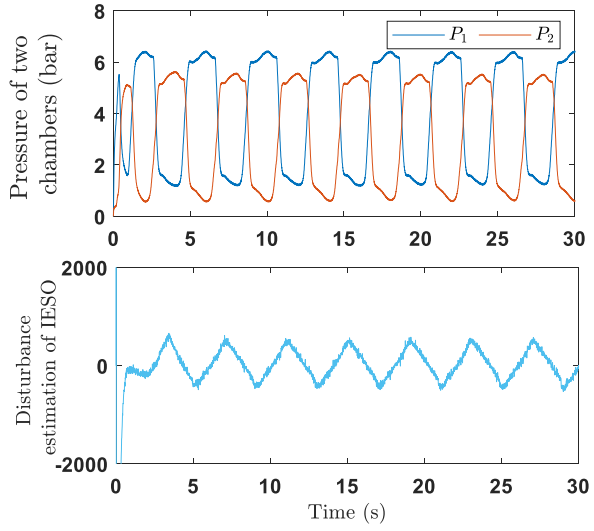

FIGURE 11. Pressure of two chamber and lumped disturbance of the suggested method in experiment.

exhibited in Tables 4 with two indexes, i.e., maximum error (MAE) and root mean square error (RMSE).

TABLE 4. Performance indices of various controllers in three experiments.

	Method	PID	PIDFF	ASMC	BCESO	Proposed
Exp. 1	RMSE	1.094	1.086	1.114	1.105	0.324
	MAE	4.077	3.730	4.046	3.981	1.348
Exp. 2	RMSE	1.184	1.116	1.146	1.145	0.669
	MAE	2.728	2.714	2.589	2.442	1.958
Exp. 3	RMSE	1.149	1.118	1.156	1.137	0.564
	MAE	3.265	2.686	3.824	2.783	1.785

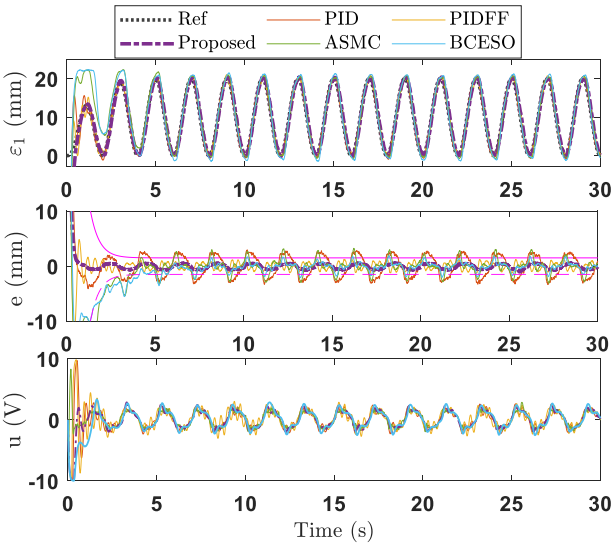

FIGURE 12. Efficiency of various control methods in experiment 3.

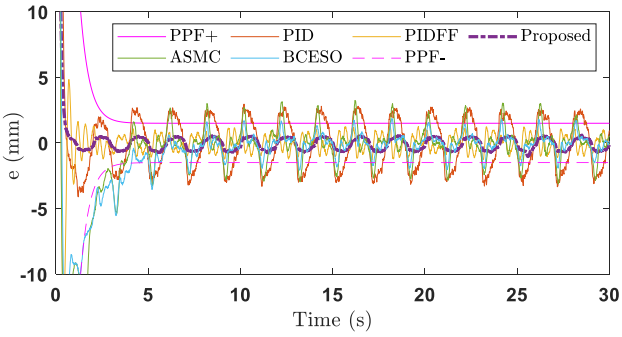

FIGURE 13. Tracking errors of various control methods in experiment 3.

The results achieved from three scenarios imply that the proposed control algorithm outperforms the other path-baseline controllers for ELHSs, particularly in terms of the performance indexes. Moreover, the experimental results imply that the suggested methodology obtains satisfactory control precision with specified performance, finite-time convergence, and quick compensation capability for the lumped disturbances.

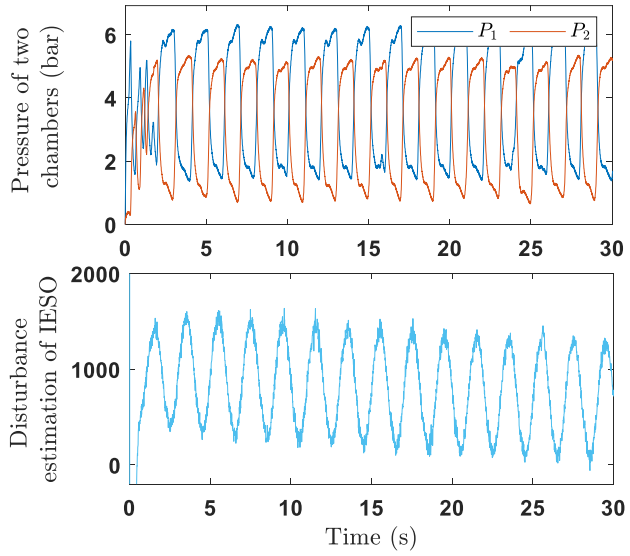

FIGURE 14. Pressure of two chamber and lumped disturbance of the suggested method in experiment.

V. CONCLUSION

In this paper, the issue of following control for an ELHS with prescribed performance and finite-time convergence was investigated. To this aim, an enhanced disturbance observer-based finite-time tracking controller with specified performance was constructed for the ELHS in the presence of lumped disturbance. Firstly, the EDO was utilized to address the lumped uncertainties, where disturbances were estimated by the EDO, taking into account the boundedness of observation errors. For the main controller, the GISMC was introduced to boost global robustness, reduce chattering and the significant effects of estimated disturbances error. The outcomes of the experiment were utilized to effectively showcase the remarkable tracking accuracy and system stability, even under adverse conditions. Future works will concentrate on the fixed-time event-triggered adaptive control of ELHS in the presence of actuator faults.

REFERENCES

[1] J. J. Eckert, T. P. Barbosa, F. L. Silva, V. R. Roso, L. C. A. Silva, and L. A. R. da Silva, "Optimum fuzzy logic controller applied to a hybrid hydraulic vehicle to minimize fuel consumption and emissions," *Expert Syst. Appl.*, vol. 207, Nov. 2022, Art. no. 117903.

[2] H. V. Dao, S. Na, D. G. Nguyen, and K. K. Ahn, "High accuracy contouring control of an excavator for surface flattening tasks based on extended state observer and task coordinate frame approach," *Autom. Construct.*, vol. 130, Oct. 2021, Art. no. 103845.

[3] T. X. Dinh, T. D. Thien, T. H. V. Anh, and K. K. Ahn, "Disturbance observer based finite time trajectory tracking control for a 3 DOF hydraulic manipulator including actuator dynamics," *IEEE Access*, vol. 6, pp. 36798–36809, 2018.

[4] C. Wang, Z. Jiao, and L. Quan, "Nonlinear robust dual-loop control for electro-hydraulic load simulator," *ISA Trans.*, vol. 59, pp. 280–289, Nov. 2015.

[5] G. Filo, "A review of fuzzy logic method development in hydraulic and pneumatic systems," *Energies*, vol. 16, no. 22, p. 7584, Nov. 2023.

[6] L. Lao and P. Chen, "Adaptive sliding mode control of an electro-hydraulic actuator with a Kalman extended state observer," *IEEE Access*, vol. 12, pp. 8970–8982, 2024.

[7] D. Q. Truong and K. K. Ahn, "Force control for press machines using an online smart tuning fuzzy PID based on a robust extended Kalman filter," *Expert Syst. Appl.*, vol. 38, no. 5, pp. 5879–5894, May 2011.

[8] D. X. Ba, T. Q. Dinh, J. Bae, and K. K. Ahn, "An effective disturbance-observer-based nonlinear controller for a pump-controlled hydraulic system," *IEEE/ASME Trans. Mechatronics*, vol. 25, no. 1, pp. 32–43, Feb. 2020.

[9] V. D. Phan, H. V. A. Truong, and K. K. Ahn, "Actuator failure compensation-based command filtered control of electro-hydraulic system with position constraint," *ISA Trans.*, vol. 134, pp. 561–572, Mar. 2023.

[10] G. Yang, H. Wang, J. Chen, and H. Zhang, "Command filtered robust control of nonlinear systems with full-state time-varying constraints and disturbances rejection," *Nonlinear Dyn.*, vol. 101, no. 4, pp. 2325–2342, Sep. 2020.

[11] C.-L. Zhang and G. Guo, "Prescribed performance fault-tolerant control of strict-feedback systems via error shifting," *IEEE Trans. Cybern.*, vol. 53, no. 12, pp. 7824–7833, 2023.

[12] Z. Xu, Q. Liu, and J. Yao, "Funnel function-based adaptive prescribed performance output feedback control of hydraulic systems with disturbance observers," *ISA Trans.*, vol. 136, pp. 701–714, May 2023.

[13] T. Berger, H. H. Lê, and T. Reis, "Funnel control for nonlinear systems with known strict relative degree," *Automatica*, vol. 87, pp. 345–357, Jan. 2018.

[14] S. Sui, Y. Yu, S. Tong, and C. L. Philip Chen, "Event-triggered robust fuzzy adaptive control for non-strict feedback nonlinear system with prescribed performance," *Appl. Math. Comput.*, vol. 474, Aug. 2024, Art. no. 128701.

[15] Z. Xu, W. Deng, H. Shen, and J. Yao, "Extended-state-observer-based adaptive prescribed performance control for hydraulic systems with full-state constraints," *IEEE/ASME Trans. Mechatronics*, vol. 27, no. 6, pp. 5615–5625, Dec. 2022.

[16] V. D. Phan and K. K. Ahn, "Optimized-based fault-tolerant control of an electro-hydraulic system with disturbance rejection," *Appl. Sci.*, vol. 12, no. 18, p. 9197, Sep. 2022.

[17] V. D. Phan and K. K. Ahn, "Fault-tolerant control for an electro-hydraulic servo system with sensor fault compensation and disturbance rejection," *Nonlinear Dyn.*, vol. 111, no. 11, pp. 10131–10146, Jun. 2023.

[18] J. Li, L. Zhang, S. Li, and J. Su, "A time delay estimation interpretation of extended state observer-based controller with application to structural vibration suppression," *IEEE Trans. Autom. Sci. Eng.*, vol. 21, no. 2, pp. 1965–1973, 2024.

[19] J. Fei, L. Liu, and Y. Chen, "Finite-time disturbance observer of active power filter with dynamic terminal sliding mode controller," *IEEE J. Emerg. Sel. Topics Power Electron.*, vol. 11, no. 2, pp. 1604–1615, Apr. 2023.

[20] J. Yang, S. Li, J. Su, and X. Yu, "Continuous nonsingular terminal sliding mode control for systems with mismatched disturbances," *Automatica*, vol. 49, no. 7, pp. 2287–2291, Jul. 2013.

[21] G. Yang, H. Wang, and J. Chen, "Disturbance compensation based asymptotic tracking control for nonlinear systems with mismatched modeling uncertainties," *Int. J. Robust Nonlinear Control*, vol. 31, no. 8, pp. 2993–3010, May 2021.

[22] M. H. Nguyen, H. V. Dao, and K. K. Ahn, "Extended sliding mode observer-based high-accuracy motion control for uncertain electro-hydraulic systems," *Int. J. Robust Nonlinear Control*, vol. 33, no. 2, pp. 1351–1370, Jan. 2023.

[23] W. Shen, D. Yao, C. Shen, and H. Li, "Finite-time fault-tolerant control for swashplate of integrated hydraulic transformer with uncertain mismatched interference," *IEEE Trans. Ind. Electron.*, vol. 70, no. 6, pp. 6347–6355, Jun. 2023.

[24] G. Yang and L. Cui, "Asymptotic tracking control for mismatched uncertain systems with active disturbance rejection," *Mathematics*, vol. 12, no. 3, p. 411, Jan. 2024.

[25] Z. Xu, N. Xie, H. Shen, X. Hu, and Q. Liu, "Extended state observer-based adaptive prescribed performance control for a class of nonlinear systems with full-state constraints and uncertainties," *Nonlinear Dyn.*, vol. 105, no. 1, pp. 345–358, Jul. 2021.

[26] S. Liu, L. Wang, C. Li, Q. Sun, Z. Chen, M. Sun, and X. Zeng, "Disturbance rejection control with voltage constraint for electro-hydraulic system involving unknown dead-zones and drastic supply pressure variation," *IEEE Access*, vol. 8, pp. 84551–84568, 2020.

[27] Q. Guo, Z. Chen, Y. Yan, and D. Jiang, "Terminal sliding mode velocity control of the electro-hydraulic actuator with lumped uncertainty," *Aerosp. Syst.*, vol. 4, no. 4, pp. 345–352, Dec. 2021.

[28] V. D. Phan, C. P. Vo, H. V. Dao, and K. K. Ahn, "Robust fault-tolerant control of an electro-hydraulic actuator with a novel nonlinear unknown input observer," *IEEE Access*, vol. 9, pp. 30750–30760, 2021.
[29] C. Wang, J. Wang, Q. Guo, X. Ren, Y. Cao, and D. Jiang, "Fixed-time adaptive neural control of electro-hydraulic system with model uncertainties: Theory and experiments," *Control Eng. Pract.*, vol. 147, Jun. 2024, Art. no. 105931.
[30] Z. Zhang, Y. Guo, D. Gong, and J. Liu, "Global integral sliding-mode control with improved nonlinear extended state observer for rotary tracking of a hydraulic roofbolter," *IEEE/ASME Trans. Mechatronics*, vol. 28, no. 1, pp. 483–494, Feb. 2023.
[31] Z. Zhang, Y. Guo, D. Gong, and S. Zhu, "Improved extended state observer-based global sliding-mode finite-time control for displacement tracking of a hydraulic roofbolter," *Nonlinear Dyn.*, vol. 111, no. 12, pp. 11191–11203, Jun. 2023.
[32] H. Razmjooei, G. Palli, and M. Nazari, "Disturbance observer-based nonlinear feedback control for position tracking of electro-hydraulic systems in a finite time," *Eur. J. Control*, vol. 67, Sep. 2022, Art. no. 100659.
[33] S. Li, Q. Guo, and Y. Yan, "Terminal sliding mode observer based dynamic surface quasi-synchronization control of multiple electro-hydraulic systems under compositive outputs constraint," *Int. J. Robust Nonlinear Control*, vol. 33, no. 12, pp. 6576–6596, Aug. 2023.
[34] B. Wang, M. Iwasaki, and J. Yu, "Finite-time command-filtered backstepping control for dual-motor servo systems with LuGre friction," *IEEE Trans. Ind. Informat.*, vol. 19, no. 5, pp. 6376–6386, May 2023.
[35] A. Levant, "Robust exact differentiation via sliding mode technique," *Automatica*, vol. 34, no. 3, pp. 379–384, Mar. 1998.
[36] M. Van, S. S. Ge, and H. Ren, "Finite time fault tolerant control for robot manipulators using time delay estimation and continuous nonsingular fast terminal sliding mode control," *IEEE Trans. Cybern.*, vol. 47, no. 7, pp. 1681–1693, Jul. 2017.
[37] Y. Wei, L. Qian, Q. Yin, and Q. Zou, "Prescribed performance dynamic surface control of hydraulic-driven barrel servo system with disturbance compensation," *Int. J. Control, Autom. Syst.*, vol. 21, no. 1, pp. 208–220, Jan. 2023.
[38] V. D. Phan, C. P. Vo, H. V. Dao, and K. K. Ahn, "Actuator fault-tolerant control for an electro-hydraulic actuator using time delay estimation and feedback linearization," *IEEE Access*, vol. 9, pp. 107111–107123, 2021.
[39] J. Yao and W. Deng, "Active disturbance rejection adaptive control of hydraulic servo systems," *IEEE Trans. Ind. Electron.*, vol. 64, no. 10, pp. 8023–8032, Oct. 2017.
[40] M. H. Nguyen and K. K. Ahn, "Extended sliding mode observer-based output feedback control for motion tracking of electro-hydrostatic actuators," *Mathematics*, vol. 11, no. 20, p. 4324, Oct. 2023.

VAN DU PHAN received the B.S. degree in electrical engineering from Hanoi University of Science and Technology, Hanoi, Vietnam, in 2013, the M.Sc. degree in electrical engineering from Thai Nguyen University of Technology, Thai Nguyen, Vietnam, in 2017, and the Ph.D. degree from the University of Ulsan, in 2023.

Currently, he is with the School of Engineering and Technology, Vinh University. His research interests include soft robot, hydraulic systems, nonlinear control, fault tolerant control, and renewable energy (fuel cell systems).

PHUONG HO SY received the Graduate Engineering degree in electronic and telecommunications from Vinh University, in 2009, and the master's degree in automation from the Military Technical Academy, in 2012. He is currently pursuing the Ph.D. degree with the Graduate University of Sciences and Technology, Vietnam Academy of Science and Technology. He is also with the School of Engineering and Technology, Vinh University. His research interests include robotics, adaptive control, fuzzy logic and neural network control, and image processing.

KYOUNG KWAN AHN (Senior Member, IEEE) received the B.S. degree from the Department of Mechanical Engineering, Seoul National University, in 1990, the M.Sc. degree in mechanical engineering from Korea Advanced Institute of Science and Technology (KAIST), in 1992, and the Ph.D. degree from Tokyo Institute of Technology, in 1999.

Since 2000, he has been with the School of Mechanical Engineering, University of Ulsan, where he is currently a Professor and the Director of the Fluid Power Control and Machine Intelligence Laboratory. His main research interests include fluid-based triboelectric nano generator, modeling and control of fluid power systems, energy saving construction machine, hydraulic robot, and power transmission in the ocean energy. He is the author or co-author of over 190 SCI(E) articles and four books in these areas. He serves as an Editor for *International Journal of Control, Automation and Systems* and an Editorial Board Member for *Renewable Energy*, The Korean Society for Fluid Power and Construction Equipment, and *Actuators*.